

Observation of Superradiant and Subradiant Spontaneous Emission of Two Trapped Ions

R. G. DeVoe and R. G. Brewer

IBM Research Division, Almaden Research Center, 650 Harry Road,
San Jose, California 95120-6099

(Received 19 October 1995)

We report the first observation of a microscopically resolved interaction between two trapped atoms. This is also the first observation of two-ion superradiance and subradiance, the most elementary example of Dicke's theory. Its signature is the variation of the spontaneous emission decay rate of a laser-cooled two-ion crystal, +1.5% and -1.2%, as the ion-ion distance is changed from 1380 to 1540 nm, in agreement with a no-free-parameter theory. The experiment uses an ion microtrap (80 μm radius) with planar electrodes and a new few-atom technique for measuring lifetimes.

PACS numbers: 42.50.Fx, 32.80.Pj, 42.50.Vk

The study of atomic interactions often begins with a *gedanken* experiment in which two atoms are assumed to be at rest a distance R apart, free of external perturbations. Comparison to experiment then requires an average over a statistical distribution of atom-atom separations, as well as other unknown microscopic variables. In this Letter we report a laboratory realization of this *gedanken* experiment using two laser-cooled trapped ions in which for the first time the interaction is directly measured as a function of the microscopic separation R . Moreover, this apparatus enables us to test the quantum electrodynamic (QED) theory of superradiance [1] in a simple configuration which is free of the theoretical uncertainties that have limited earlier experiments [2], for example, nonlinear propagation and diffraction effects and assumptions about the coupling of N spin- $\frac{1}{2}$ systems (where $N \gg 1$). Our experiment is an optical version of the *gedanken* experiment which Dicke used to introduce the subject 40 years ago, in which the spontaneous emission of magnetic dipole radiation from two neutrons is replaced by the electric dipole radiation of two optical transitions. There is currently renewed interest in superradiance since it is expected to play a dominant role in the optical behavior of cold dense systems such as Bose-Einstein condensates [3,4].

The experiment is based on previous work in radio frequency (rf) Paul traps, single ion trapping and detection, and ion crystallization. Dehmelt [5] obtained images of laser-cooled single ions almost 20 years ago and more recently several groups [6-9] have produced ordered arrays of essentially stationary ions (ion crystals) in Paul traps. The latter offered the possibility in principle of performing a microscopically resolved experiment with only two atoms but the ions were too far apart ($>3 \mu\text{m}$) to interact. Eichmann *et al.* [10] demonstrated Bragg scattering of two trapped ions in analogy to Young's double slit experiment but again interactions could not be observed due to the large separation of $>15\lambda$, where λ is the wavelength of light. For this experiment we have developed microscopic ion traps [11,12] of "planar" geometry which

are strong enough to bring the ions to within $\approx 1 \mu\text{m}$, or 2λ , of each other. Observing superradiance has also required a precise new method [13] for measuring lifetimes of one or two atoms which has been shown to equal or exceed the statistical power of previous many-atom methods.

The principle of the experiment is to measure the spontaneous emission rate $\Gamma(R)$ of a two-ion crystal as a function of the ion-ion separation R , and to compare it to that of a single ion Γ_0 in the same apparatus. Superradiance and subradiance are detected when $\Gamma(R) > \Gamma_0$ or $\Gamma(R) < \Gamma_0$, respectively [14,15]. In Dicke's theory two interacting two-level systems are treated as a single four-level system with collective states represented by triplet $|+\rangle$ and singlet $|-\rangle$ wave functions as shown in Fig. 1. The master equation [16] or Fermi's golden rule [17] can be used to derive decay rates Γ_{\pm} to or from the $|\pm\rangle$ states (see Fig. 2) which are well approximated by

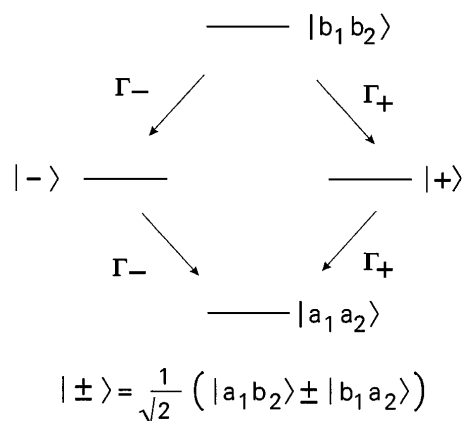


FIG. 1. Level structure of superradiant and subradiant states for two two-level atoms coupled to a common radiation field. Γ_{\pm} is the spontaneous emission rate into and out of the triplet and singlet states $|\pm\rangle$. The ground and excited states of atoms 1,2 are given by $|a_{1,2}\rangle$ and $|b_{1,2}\rangle$, respectively. The levels can also be labeled with spin 1 quantum numbers as $|b_1 b_2\rangle = |1, 1\rangle$, $|+\rangle = |1, 0\rangle$, $|a_1 a_2\rangle = |1, -1\rangle$, and $|-\rangle = |0, 0\rangle$.

$$\Gamma_{\pm}(R) = \Gamma_0 \left(1 \pm \frac{3}{2} \frac{\sin kR}{kR} + \dots \right) \quad (1)$$

in the region $kR > 10$ used in our experiment, where $k = 2\pi/\lambda$ and the laser polarization \vec{E}_l has been chosen so that $\vec{E}_l \cdot \vec{R} = 0$. Γ is measured by a transient technique in which the ion crystal is excited by a short laser pulse at $t = 0$ and the time of arrival of spontaneous photons is recorded on a time-to-digital converter (TDC), which yields a decay curve (histogram) proportional to $W(R, t)$ representing the sum of all four transitions in Fig. 1,

$$W(R, t) = \rho_e(t) [\Gamma_+(R) + \Gamma_-(R)] + \rho_+(t)\Gamma_+(R) + \rho_-(t)\Gamma_-(R), \quad (2)$$

where the diagonal density matrix elements are denoted by a single subscript, e.g., $\rho_+ \equiv \rho_{++}$, $|e\rangle \equiv |b_1b_2\rangle$, and $|g\rangle \equiv |a_1a_2\rangle$. The time-dependent $\rho(t)$ are given by the master equation which reduces to a set of rate equations as represented by arrows in Fig. 1, for example, $d\rho_+/dt = \Gamma_+\rho_e - \Gamma_+\rho_+$. In the region $kR \leq 1$ superradiance is easily identified since $W(R, t)$ is a multiexponential with both fast and slow components [2]. However, in our case $kR \approx 10$ and $|\Gamma_{\pm} - \Gamma_0| < \Gamma_0/10$ so that super- and subradiant decays are difficult to distinguish. Observation of a strong signal requires separate excitation of either the singlet or triplet state and that ρ_e be essentially empty, to avoid the $\Gamma_+ + \Gamma_- = 2\Gamma_0$ term in Eq. (2) which dilutes the signal.

Selective population of the $|\pm\rangle$ states is achieved by coherent excitation with the geometry of Fig. 3. The laser pulse with wave vector \vec{k} induces dipole moments in atoms 1 and 2 with a phase difference $\Phi = \vec{k} \cdot \vec{R}$ where $\rho_{ab}^1 = \rho_{ab}^2 e^{i\Phi}$. The populations of the $|\pm\rangle$ states can be expressed in terms of the single-atom density matrices ρ [1,2] by

$$\rho_{\pm} = \frac{1}{2} [\rho_{aa}^1 \rho_{bb}^2 + \rho_{bb}^1 \rho_{aa}^2 \pm (\rho_{ab}^1 \rho_{ba}^2 + \rho_{ba}^1 \rho_{ab}^2)], \quad (3)$$

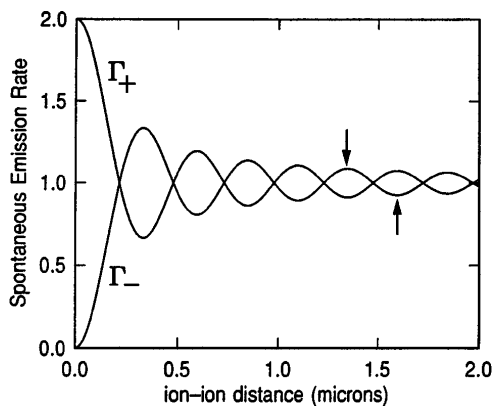


FIG. 2. Plot of the relative decay rate Γ_{\pm}/Γ_0 for two two-level atoms as a function of separation R , for $\lambda = 493$ nm. The arrows mark the part of the Γ_- curve explored by the experiment.

which can be derived by transforming from the direct product representation $\rho' = \rho^1 \otimes \rho^2$ to the (unprimed) representation of Fig. 1 using $\rho = U^{-1}\rho'U$, where U is a trivial unitary transformation. Equation (3) reduces to

$$\rho_{\pm} = |\rho_{ab}|^2 [1 \pm \cos \Phi] \quad (4)$$

for fully coherent excitation where $|\rho_{ab}|^2 = \rho_{aa}\rho_{bb}$. Hence essentially all the excitation can be placed in either the $|+\rangle$ or the $|-\rangle$ state by adjusting R and θ to set the excitation phase $\Phi = 0$ or π , respectively. The population of the excited state can be neglected for weak excitation since $\rho_e \rightarrow |\rho_{ab}|^4$ in this limit. In the general case, both $|+\rangle$ and $|-\rangle$ states will be excited and solution of Eq. (2) shows that $W(R, t)$ approximates a single exponential decay with rate

$$\Gamma(R) = \Gamma_0 [1 + \alpha \cos(\Phi) \sin(kR)/kR + \dots], \quad (5)$$

where $\alpha = \frac{3}{2}$ for two-level systems. This is consistent with a simple physical picture [15] in which spontaneous emission is enhanced when the atoms' dipole moments are in phase and inhibited when they are out of phase, allowing for retardation. Level degeneracy reduces α from $\frac{3}{2}$ to $\frac{1}{2}$ in our experiment. We measure $\Gamma(R)$ of the $6^2P_{1/2}$ to $6^2S_{1/2}$ transition in Ba_{138}^+ which has twofold degenerate $m_J = \pm \frac{1}{2}$ ground and excited states. The presence of both $\Delta m = 0$ and $\Delta m = \pm 1$ decays for each excited state leads to a loss of coherence as predicted in theoretical studies of resonance fluorescence [18] and observed in two-ion interference experiments [10]. $\alpha = \frac{1}{2}$ results from averaging the superradiant matrix elements in Fermi's golden rule [17] over the relevant $\Delta m = 0$ and $\Delta m = \pm 1$ transitions. Loss of coherence due to micromotion Doppler shifts yields an additional factor $J_0^2(z) - 2J_1^2(z) + \dots = 0.65$, where J_n is the Bessel function of order n , $z = ka$, a is the amplitude of the ion micromotion, and $z = 0.60$ for our conditions. Thermal motion of the ions is negligible compared to micromotion since at the Doppler limit the residual motion is < 10 nm rms. The final result of the

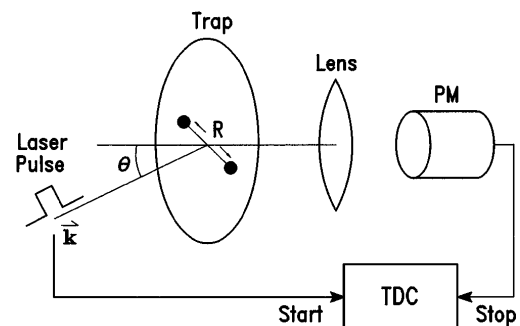


FIG. 3. Diagram of the experiment. A two-ion crystal is condensed in the radial plane of an $80 \mu\text{m}$ radius planar ion trap (here shown schematically by a ring). The laser beam makes an angle θ to the trap axis and excites the crystal at $t = 0$. The time of arrival of the spontaneous photons is recorded on a time-to-digital converter (TDC), which is fit to an exponential decay.

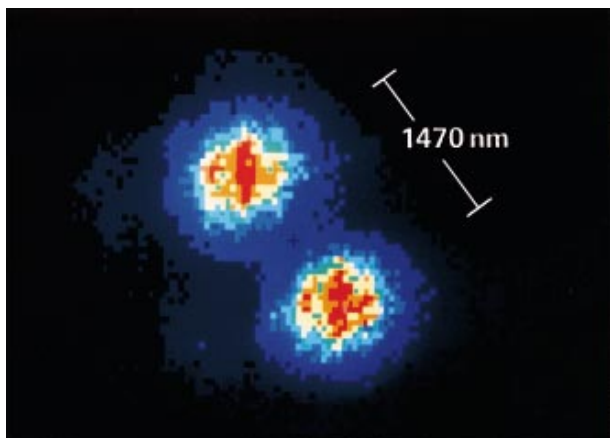


FIG. 4. (color) Diffraction-limited image of a two-ion crystal with $R = 1470$ nm. This determines the orientation of the interatomic vector R enabling a no-free-parameter fit.

theory is $\alpha = 0.33$. See Ref. [19] for a master equation treatment of two interacting four-level systems.

The apparatus is shown in Fig. 3. The novel features are the microtrap and the lifetime measuring system. The planar ion trap [11,12] produces a quadrupole field from flat electrodes with concentric circular apertures. It is constructed from three $25 \mu\text{m}$ thick Be-Cu foils spaced $100 \mu\text{m}$ apart containing a central trapping aperture of $80 \mu\text{m}$ radius. The two-ion crystals are produced at a nominal ion-ion spacing of 1470 nm when driven with an ≈ 500 V peak at 93.5 MHz, as determined by measuring the secular oscillation frequency of a single ion, 4.00 MHz. dc voltages of -10 and $+5$ V were applied to change the ion-ion spacing R to 1380 and 1540 nm, respectively. The Ba_{138}^+ ions are laser cooled as in a previous work [8] using two frequency stabilized

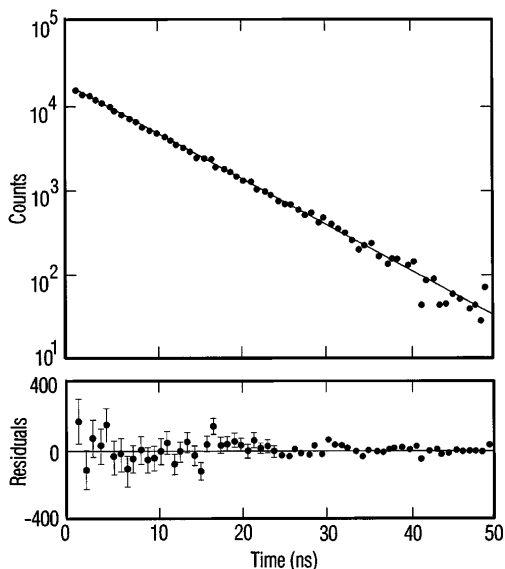


FIG. 5. Three-parameter fit (solid line) of five combined data sets at $R = 1380$ nm, showing residuals (lower figure). The fit yields a superradiant lifetime of 7.820 ± 0.074 ns, a $\chi^2 = 67$ for 65 degrees of freedom, and a probability $P(\chi^2 | n) = 0.32$.

cw dye lasers exciting the $6^2P_{1/2}$ to $6^2S_{1/2}$ transition at 493 nm and the $6^2P_{1/2}$ to $5^2D_{3/2}$ transition at 650 nm. Both laser beams were focused to a beam waist radius of about $15 \mu\text{m}$ with powers of 500 to 1000 nW. The crystal is viewed through a 2 mm sapphire UHV window by a microscope objective which is compensated for the spherical aberration of the window, yielding diffraction-limited images as in Fig. 4. The figure shows that the crystal is inclined at an angle $\varphi = 40^\circ$ to the (horizontal) plane containing \vec{k} and the trap axis, which determines the excitation phase $\Phi = kR \sin \theta \sin \varphi \approx \pi$ for $R \approx 1470$ nm and $\theta = 16^\circ$. The crystal is therefore predominantly excited into the antisymmetric $|- \rangle$ state. The ion crystal lifetime is measured by a single-photon counting technique which records the arrival time of the spontaneous photons on a TDC. A measurement cycle was repeated every 250 ns, of which the first 160 ns was devoted to laser cooling the ions. Both red and blue lasers were then turned off for 30 ns to allow the $6P$ state to relax to the ground state. The blue laser was turned on for 6 ns to excite the $|\pm \rangle$ collective states and the 493 nm spontaneous emission was monitored for the next 50 ns. The pulses were generated by two *nonlinear* electro-optic modulators [13] with a 2 ns rise time and >60 db on-off ratio. The imaging photomultiplier produced a fast timing output from the multichannel plate intensifier which was used to trigger the TDS. The resulting histogram (see Fig. 5) was fit to a decay of the form $A \exp(-\Gamma t) + B$ using a nonlinear least-squares routine [20]. We have shown elsewhere [13] how the use of only one or two atoms can provide *greater* statistical power than conventional many-atom methods by avoiding a systematic error (pulse pileup) due to the fluctuations in the number of decaying atoms.

Figure 6 shows the variation of the ion crystal lifetime $\tau = 1/\Gamma$ with R in agreement with the no-free-parameter theory of Eq. (5). Measurements at $R = 1380$, 1470 , and

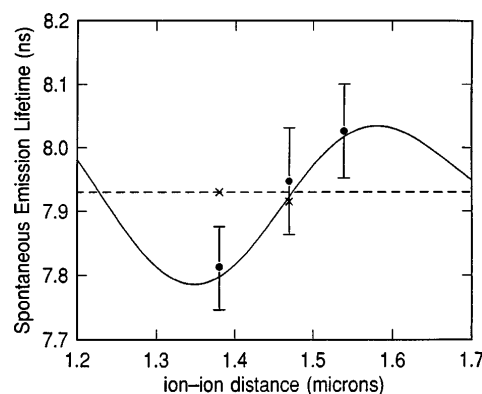


FIG. 6. Comparison of theory to experimental points at 1380 , 1470 , and 1540 nm (see text). The ion-ion distance is independently known by measuring the secular oscillation frequency of one ion. The lifetime is calibrated by comparison to 7.930 ± 0.03 ns measured for a single ion in the same apparatus. Note the polarization sensitivity (crosses, with error bars omitted for clarity).

1540 nm yield lifetimes of $\tau = 7.813 \pm 0.67$ ns, 7.947 ± 0.084 ns, and 8.026 ± 0.074 ns, respectively, where the errors are 1σ (standard deviation). Separate measurements of one ion gave $\tau = 7.930 \pm 0.03$ ns (dotted line). The superradiant point at 1380 nm is $1.5\% \pm 0.8\%$ below the single-ion value (-1.7σ) while the subradiant point at 1540 nm is $1.2\% \pm 0.9\%$ above it ($+1.3\sigma$). The three data points fit the theory with a probability $P = 0.64$ while a fit to the 7.930 ns single-ion value gives $P < 0.005$ (a 3σ effect), taking account of the signs. A variety of statistical and systematic tests has been used to confirm these results. High statistics measurements of τ of a single ion were made to rule out systematic effects due to rf trap voltage, total count rate, laser polarization, magnetic field, etc. The data points shown in Fig. 6 were averaged from a total of 36 runs made on an ion crystal which was continuously observed for 11 h, during which the laser tuning and power levels were held constant to minimize systematic shifts. Similar superradiance signals have been observed on other days but the ion crystals were lost after a few hours so that the full R and polarization dependence could not be mapped out under constant conditions. The ion-ion distance was varied by changing the dc voltage on the trap while leaving the rf voltage constant, which minimized potential systematic errors due to rf pickup or micromotion. τ and χ^2 were computed for each of the 36 runs and their distributions were found to be nearly ideal. For example, χ^2/n ranged from a low of 0.48 to a high of 1.37 and a histogram of the probability [20] $P(\chi^2 | n)$ is flat between 0 and 1, e.g., five runs have $0 < P < 0.1$ and five runs have $0.9 < P < 1.0$. No runs were excluded for bad χ^2 , no outliers were observed, and individual values of τ are consistent with the averages. Specifically, seven of the eight runs that comprise the subradiant point lie above the one-ion value while all ten superradiant runs lie below it. As a final test, the polarization of the exciting laser was varied without changing any other experimental parameters using an electronic liquid crystal rotator. Theory [15–17,19] shows that superradiant effects are reduced by a factor $kR > 10$ when the polarization $\vec{E}_l \parallel \vec{R}$ instead of $\vec{E}_l \perp \vec{R}$ as assumed in Eq. (1). Data taken at the superradiant $R = 1380$ nm with $\vec{E}_l \parallel \vec{R}$ (crosses in Fig. 6) yield $\tau = 7.930 \pm 0.065$ ns, or $0.0 \pm 0.8\%$ relative to one ion, compared to a -1.5% signal for the correct polarization. This shows that the signal has the polarization sensitivity expected from Dicke's theory.

In these initial experiments superradiance has been detected with 3σ resolution, but the apparatus is designed to be scaled into the region $100 \text{ nm} < R < 1000 \text{ nm}$ where superradiance dominates spontaneous emission and $\Gamma_+/\Gamma_- > 2$. The planar trap is designed for photolithographic microfabrication [11,12] at dimensions of $10\text{--}20 \mu\text{m}$ where $R \rightarrow 100 \text{ nm}$. The first photolithographic devices have been constructed. The few-atom lifetime technique can also be developed towards its theoretical

resolution of about 0.1% σ per minute of integration time [13]. In this regime superradiance may be resolved with high precision to test predictions [2] of such effects as van der Waals dephasing, multiexponential decay, and crystal shape dependence which are inaccessible to conventional experiments.

In conclusion we have demonstrated that atom-by-atom studies of atomic interactions are practical. The use of ion traps permits precise control of ion-ion distances so that the R dependence may be observed directly. This opens the door for new types of microscopically resolved, detailed, and precise tests of QED and other atomic interactions.

The authors thank L. Young of Argonne National Laboratory for assistance with the time-resolved single-photon counting technique and for a critical reading of the manuscript.

-
- [1] R. H. Dicke, *Phys. Rev.* **93**, 99 (1954).
 - [2] M. Gross and S. Haroche, *Phys. Rep.* **93**, 301 (1982).
 - [3] M. H. Anderson, J. R. Ensher, M. R. Matthews, C. E. Wieman, and E. A. Cornell, *Science* **269**, 198 (1995).
 - [4] C. C. Bradley, C. A. Sackett, J. J. Tollet, and R. G. Hulet, *Phys. Rev. Lett.* **75**, 1687 (1995).
 - [5] H. Dehmelt, *Rev. Mod. Phys.* **62**, 525 (1990).
 - [6] F. Diedrich, E. Peik, J. M. Chen, W. Quint, and H. Walther, *Phys. Rev. Lett.* **59**, 2931 (1987).
 - [7] D. J. Wineland, J. C. Bergquist, W. M. Itano, J. J. Bollinger, and C. H. Manning, *Phys. Rev. Lett.* **59**, 2935 (1987).
 - [8] J. Hoffnagle, R. G. DeVoe, L. Reyna, and R. G. Brewer, *Phys. Rev. Lett.* **61**, 255 (1988).
 - [9] T. Sauter, H. Gilhaus, I. Siemers, R. Blatt, W. Neuhauser, and P. Toschek, *Z. Phys. D* **10**, 153 (1988).
 - [10] U. Eichmann, J. C. Bergquist, J. J. Bollinger, W. M. Itano, and D. J. Wineland, *Phys. Rev. Lett.* **70**, 2359 (1993).
 - [11] R. G. Brewer, R. G. DeVoe, and R. Kallenbach, *Phys. Rev. A* **46**, 4781 (1992).
 - [12] R. G. Brewer, R. G. DeVoe, K. L. Foster, and J. A. Hoffnagle, U.S. Patent No. 5,248,883; U.S. Patent No. 5,379,000.
 - [13] R. G. DeVoe and R. G. Brewer, *Opt. Lett.* **19**, 1891 (1994).
 - [14] R. G. DeVoe and R. G. Brewer, in *Proceedings of the Twelfth International Conference on Laser Spectroscopy* (World Scientific, Singapore, to be published).
 - [15] R. G. DeVoe, in "Quantum Dynamics of Simple Systems, Scottish Universities Summer School in Physics 44" (Springer, New York, to be published).
 - [16] G. S. Agarwal, *Quantum Optics*, Springer Tracts in Modern Physics Vol. 70 (Springer-Verlag, Berlin, 1974).
 - [17] E. A. Power, *J. Chem. Phys.* **46**, 4297 (1967).
 - [18] D. Polder and M. Schuurmans, *Phys. Rev. A* **14**, 1468 (1976).
 - [19] R. G. Brewer, *Phys. Rev. A* **52**, 2965 (1995).
 - [20] W. Press, B. Flannery, S. Teukolsky, and W. Vetterling, *Numerical Recipes* (Cambridge University Press, New York, 1986).